Kundrot, C. E., & Richards, F. M. (1987) *J. Mol. Biol. 193*, 157.
Loll, P. J., & Lattman, E. E. (1989) *Proteins: Struct., Funct., Genet. 5*, 183.
Luzatti, P. V. (1952) *Acta Crystallogr. 5*, 802.
Mehdi, S., & Gerlt, J. A. (1982) *J. Am. Chem. Soc. 104*, 3223.
Sheriff, S., & Hendrickson, W. A. (1987) *Acta Crystallogr. A43*, 118.
Steigemann, W. (1974) Die Entwicklung und Anwendung von Rechenverfahren und Rechenprogrammen zur Stukturanalyse von Proteinen am Beispiel des Trypsin-Trypsinhibitor Komplexes, des freien Inhibitors und der L-Asparaginase, Ph.D. Thesis, Technical University of Munich.
Takahara, M., Hibler, D. W., Barr, P. J., Gerlt, J. A., & Inouye, M. (1985) *J. Biol. Chem. 260*, 2670.
Wilde, J. A., Bolton, P. H., Dell'Acqua, M., Hibler, D. W., Pourmotabbed, T., & Gerlt, J. A. (1988) *Biochemistry 27*, 4127.

Solid-State ^{13}C and ^{15}N NMR Study of the Low pH Forms of Bacteriorhodopsin†

Huub J. M. de Groot,‡,§,‖ Steven O. Smith,‡,⊥ Jacques Courtin,§ Ellen van den Berg,§ Chris Winkel,§ Johan Lugtenburg,§ Robert G. Griffin,‡ and Judith Herzfeld*,‖

Francis Bitter National Magnet Laboratory, Massachusetts Institute of Technology, Cambridge, Massachusetts 02139, Gorlaeus Laboratoria der Rijksuniversiteit te Leiden, 2300 RA Leiden, The Netherlands, and Department of Chemistry, Brandeis University, Waltham, Massachusetts 02254

Received September 11, 1989; Revised Manuscript Received February 13, 1990

ABSTRACT: The visible absorption of bacteriorhodopsin (bR) is highly sensitive to pH, the maximum shifting from 568 nm (pH 7) to ~600 nm (pH 2) and back to 565 nm (pH 0) as the pH is decreased further with HCl. Blue membrane (λ_{max} >600 nm) is also formed by deionization of neutral purple membrane suspensions. Low-temperature, magic angle spinning ^{13}C and ^{15}N NMR was used to investigate the transitions to the blue and acid purple states. The ^{15}N NMR studies involved [ϵ-^{15}N]lysine bR, allowing a detailed investigation of effects at the Schiff base nitrogen. The ^{15}N resonance shifts ~16 ppm upfield in the neutral purple to blue transition and returns to its original value in the blue to acid purple transition. Thus, the ^{15}N shift correlates directly with the color changes, suggesting an important contribution of the Schiff base counterion to the "opsin shift". The results indicate weaker hydrogen bonding in the blue form than in the two purple forms and permit a determination of the contribution of the weak hydrogen bonding to the opsin shift at a neutral pH of ~2000 cm^{-1}. An explanation of the mechanism of the purple to blue to purple transition is given in terms of the complex counterion model. The ^{13}C NMR experiments were performed on samples specifically ^{13}C labeled at the C-5, C-12, C-13, C-14, or C-15 positions in the retinylidene chromophore. The effects of the purple to blue to purple transitions on the isotropic chemical shifts for the various ^{13}C resonances are relatively small. It appears that bR_{600} consists of at least four different species. The data confirm the presence of 13-*cis*- and *all-trans*-retinal in the blue form, as in neutral purple dark-adapted bR. All spectra of the blue and acid purple bR show substantial inhomogeneous broadening which indicates additional irregular distortions of the protein lattice. The amount of distortion correlates with the variation of the pH, and not with the color change.

Bacteriorhodopsin (bR),[1] the purple membrane protein of the halophilic bacterium *Halobacterium halobium* (Oesterhelt & Stoeckenius, 1971, 1973a; Lozier et al., 1975), works as a light-driven proton pump, establishing a proton gradient across the cell membrane [for a review, see, e.g., Stoeckenius and Bogomolni (1982)]. While the detailed 3D structure of bR is unknown, it has been established that the protein consists of a single polypeptide chain (Khorana et al., 1979; Ovchinikov et al., 1977, 1979) that is believed to be folded into seven transmembrane segments (Henderson & Unwin, 1975) surrounding the retinylidene chromophore.

One of the remarkable features of bR is the relatively large (5100 cm^{-1} at neutral pH) protein-induced shift of the absorption maximum (λ_{max}) of the chromophore, which is responsible for its characteristic purple color. This spectral shift, commonly referred to as the opsin shift, is defined as the

† This research was supported by the National Institutes of Health (GM-23289, GM-36810, and RR-00995), the "stichting Scheikundig Onderzoek Nederland" (SON, Netherlands Foundation for Chemical Research), and the "Nederlandse Organisatie voor Wetenschappelijk Onderzoek" (NWO, Netherlands Organization for the Advancement of Scientific Research). H.J.M.d.G. is a recipient of an NWO fellowship (S81-346) and a research career development fellowship (Akademie-Onderzoeker) from the "Koninklijke Nederlandse Akademie van Wetenschappen (Royal Dutch Academy of Sciences). S.O.S. was supported by an NIH postdoctoral fellowship (GM-10502).

‡ Massachusetts Institute of Technology.
§ Gorlaeus Laboratoria der Rijksuniversiteit te Leiden.
‖ Brandeis University.
⊥ Present address: Department of Molecular Biophysics and Biochemistry, Yale University, New Haven, CT 06511.

[1] Abbreviations: bR, bacteriorhodopsin; bR_{560}, dark-adapted bR comprising a mixture of bR_{555} and bR_{568} (Scherrer et al., 1989); bR_{555}, 13-cis component of dark-adapted bR; bR_{568}, light-adapted bR; bR_{600}, blue membrane obtained by acidification or deionization of bR_{560}; bR_{565}, acid purple membrane obtained by acidification of blue membrane with HCl; CP, cross-polarization; *f*, fraction of total intensity in the difference spectrum; FWHM, full width at half-maximum; MAS, magic angle spinning; PSB, protonated Schiff base; PM, purple membrane; ppm, parts per million; TMS, tetramethylsilane; λ_{max}, wavelength of maximum visible absorption; ω_r, magic angle spinning speed; σ, chemical shift.

0006-2960/90/0429-6873$02.50/0

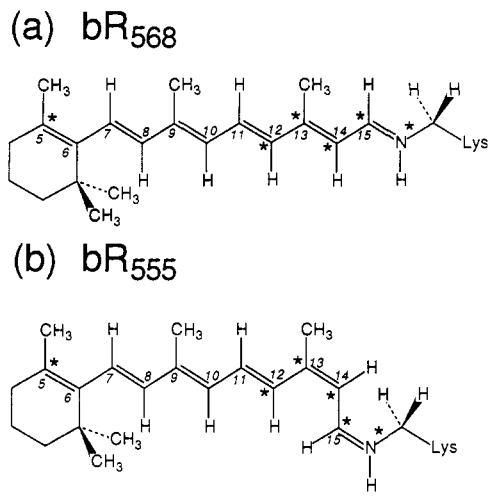

FIGURE 1: Dark-adapted bR (bR_{560}) consists of a ~4:6 mixture of bR_{568} and bR_{555}, with different chromophore structures. Comparable structures are found in bR_{600}. The positions of the labels studied in this work are marked with an asterisk.

difference between the energies of maximum visible absorption of the free protonated retinal Schiff base in solution (λ_{max}^{-1} 22 700 cm^{-1}) and the light-adapted retinal–protein complex (λ_{max}^{-1} 17 600 cm^{-1}). There have been numerous investigations of the opsin shift (Honig et al., 1976; Nakanishi et al., 1980; Bagley et al., 1982; Rothschild & Marrero, 1982; Harbison et al., 1983, 1985a,b; Hildebrandt & Stockburger, 1984; Lugtenburg et al., 1986; Spudich et al., 1986; Smith et al., 1987), and currently, the effect is thought to be due to a combination of various chromophore–protein interactions (Muradin-Szweykowska et al., 1984; Lugtenburg et al., 1986). Important contributions include a weak hydrogen bond between the protonated Schiff base and its counterion (Oseroff & Callender, 1974; Blatz & Mohler, 1975; Harbison et al., 1983; de Groot et al., 1989) and isomerization of the C_6–C_7 bond from the 6-s-cis structure dominating in solution to the 6-s-trans bR geometry illustrated in Figure 1 (Harbison et al., 1985a,b).

It has been shown that deionization or acidification considerably affects the opsin shift. When cations are removed, the opsin shift increases, and the color changes from purple to blue (Kimura al., 1984; Chang et al., 1985). This additional red shift amounts to ~940 cm^{-1}, yielding a species with λ_{max} >600 nm (bR_{600}). The same color change is observed when the pH is decreased to 2. This similarity between the spectral effects of deionization and acidification to pH 2 (Chang et al., 1985) and the close correspondence of the chromophore structures for these two forms of the membrane (Smith & Mathies, 1985; Massig et al., 1985) indicate that deionization and acidification to pH 2 result in equivalent proton–cation exchange at the membrane. However, further acidification of blue membrane reverses the color change. In particular, acidification with HCl yields a purple pigment with λ_{max} = 565 nm (bR_{565}) at pH 0.

Studies of the neutral purple to blue transition have been reviewed and analyzed in detail by Szundi and Stoeckenius (1989). They conclude that this color change is controlled by surface pH with an apparent p*K* of ~1.7. Changes in surface pH may affect the chromophore in various ways. Of particular interest is the possibility that changes occur in the protonation of the Schiff base (Fischer & Oesterhelt, 1979; Mowery et al., 1979; Smith & Mathies, 1985). Thus, a detailed investigation of the purple to blue transition may lead to a better understanding of at least one of the important mechanisms that contributes to the opsin shift.

In order to probe the effects of deionization and acidification on the chromophore, we have investigated a set of samples specifically labeled at key positions in the conjugated system of the retinals, which are marked with asterisks in Figure 1. Our main effort concentrates on the Schiff base nitrogen and the adjacent conjugated carbons. As was demonstrated previously in a series of detailed NMR investigations of bR_{560} and PSB model compounds (Harbison et al., 1983b, 1985a,b; Smith et al., 1989), the largest differences in isotropic chemical shift, between the bR chromophore and the PSB retinylidene-*N*-butylammonium chloride, are encountered at the ends of the conjugated system (i.e., for the Schiff base nitrogen and for the C-5 position of the ionone ring). The NMR chemical shift reflects variations in electron density, which in turn are related to optical properties. Therefore, the strength of the hydrogen bond between the protonated Schiff base nitrogen and its associated counterion was considered an important factor in the establishment of the opsin shift.

This idea is supported by the results of the present study. By far, the largest effects of the purple to blue to purple transitions are observed at the Schiff base nitrogen, which moves ~16 ppm upfield in the neutral purple to blue transition, and by the same amount downfield in the blue to acid purple transition. Accompanying this change in the ^{15}N resonance position is an ~5 ppm downfield movement of the ^{13}C-5 line. The variations of all other retinal ^{13}C shifts which have been studied are smaller. The changes in the ^{15}N chemical shift correlate well with changes in the optical spectra and permit us to assess the contribution of the weak hydrogen bond to the opsin shift in bR. Of the 5100 cm^{-1} shift, about 2000 cm^{-1} can be attributed to the weak hydrogen bond. In addition, we observe an overall line broadening in the ^{13}C and ^{15}N spectra, which suggests distortions of the protein lattice adjacent to the chromophore in the blue and acid purple forms. We also find that the blue membrane contains a mixture of at least four different species, two of which have a 15-anti chromophore while the other two contain a 15-syn chromophore (as compared to a single species of each type in dark-adapted PM).

Materials and Methods

PM was obtained from a culture of the JW-3 strain by using the purification procedure of Oesterhelt and Stoeckenius (1973). The synthesis of the labeled retinals, enriched to approximately 90%, was performed following procedures described elsewhere (Pardoen et al., 1984, 1985; Courtin et al., 1985). Regeneration of PM with labeled retinals was carried out following a procedure similar to that of Smith et al. (1989). PM fragments were suspended in a 0.5 M hydroxylamine solution which was titrated to pH 7.9–8.0 with KOH. Bleaching to ~95% was accomplished in the dark overnight at ~35 °C and was monitored by following changes in the absorption spectrum. The bleached solutions were washed (1×) with water or 10 mM HEPES solution and regenerated with a slight excess of the labeled retinals. The retinal was dissolved in a minimum amount of ethanol before being added to the bleached membrane. (It is important to use very small amounts of ethanol because it strongly affects the efficiency of the regeneration.) The excess retinal, together with retinaloxime generated by the bleaching procedure, was removed by extensive washing (10–15×) with 2% aqueous solutions of bovine serum albumin (Sigma Chemical Co., St. Louis, MO). The efficiency of regeneration was checked in each case by comparing the intensity ratios of the 280-nm and 560-nm peaks in the bR absorption spectrum before and after regeneration.

Typically, the regeneration efficiencies were 90–95%.

[ϵ-^{15}N]Lysine bR was prepared by growing *Halobacterium halobium* JW-3 on a synthetic medium containing [ϵ-^{15}N]-lysine, according to procedures described previously by Argade et al. (1981). Incorporation was verified with a [^3H]lysine tracer and was greater than 95%.

The acid blue and acid purple samples were prepared by simple addition of concentrated aqueous HCl to the PM suspensions. Deionized blue samples (λ_{max} >600 nm) were prepared by overnight dialysis of neutral purple samples in a bed of cation-exchange resin (Bio-Rad AG-50W X2), using spectroscopic-grade water (Merck) that had been deionized ($\rho > 1$ MΩ cm) by passage through a cation/anion-exchange column [Bio-Rad AG501-X8(D)]. For storage and manipulation of the blue species, we employed plastic bottles, tubes, and tools that were cleaned thoroughly with ~1 N HCl solution and deionized water. We also attempted two other deionization procedures, namely, EDTA treatment (Chang et al., 1985) and a cation-exchange column (Kimura et al., 1984). The EDTA-treated samples were indistinguishable from the dialyzed samples in the NMR. The column procedure was not successful, since the regenerated samples precipitated in the column, and the spectrum of the sample that was obtained through extensive washing appeared to be very different from those obtained for dialyzed or EDTA-treated samples. It must be noted that some precipitation of the regenerated samples also occurred during dialysis. However, this does not represent a problem as far as the solid-state NMR spectroscopy is concerned.

NMR data were collected with a home-built spectrometer and home-built probes, operating at a proton frequency of 317 MHz. The ^1H pulse length was 3 μs, and the ^{13}C and ^{15}N pulse lengths were typically 7 and 10 μs, respectively. The probes are equipped with 7-mm rotors from Doty Scientific (Columbia, SC). It should be emphasized that all the NMR experiments were performed on fully hydrated membranes, using sealed rotors.

^{13}C and ^{15}N chemical shifts are reported in ppm relative to TMS and 5.6 M $^{15}NH_4Cl$, respectively. As an internal calibration standard for the ^{13}C spectra, we used a bR peak positioned at 55.8 ppm whose position is invariant with temperature. For the ^{15}N spectra, we employed the NH_3^+ peak from the lysine side chains not involved in the Schiff base linkage (8.4 ppm).

Most experiments were carried out on ~80-mg samples at relatively low temperatures (170 K < T < 200 K), where the signal to noise ratio is enhanced. The equipment for cooling the bearing and drive gas was constructed in our laboratory and will be described elsewhere (Creuzet et al., to be published). The standard MAS technique, with cross-polarization and proton decoupling during acquisition, was used for every experiment [Andrew et al., 1958; Pines et al., 1973; also see Griffin et al. (1988)]. Recycle delays were 1–2 s, and CP mixing times were 2 ms.

In recording the ^{13}C spectra of labeled bR, extensive use was made of MAS difference spectroscopy which permits suppression of the natural-abundance background (de Groot et al., 1988), and therefore yields high-resolution spectra of only the labeled positions (i.e., one carbon in approximately 80 000[2] daltons). For the analysis of the difference spectra, we used the sideband intensities of Herzfeld and Berger (1980)

[2] Calculated as follows: bR protein (M_r ~26 000) is surrounded by lipids (~25% of sample weight). Since one easily observes the individual all-trans and 13-cis forms of dark-adapted bR, effectively one carbon is detected in an ~80 000-dalton background.

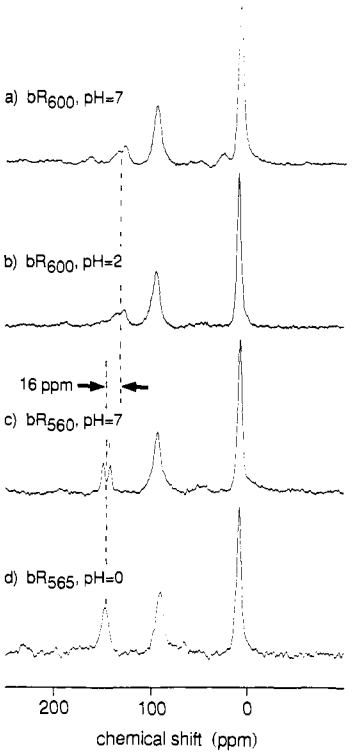

FIGURE 2: Proton-decoupled ^{15}N MAS spectra for [ϵ-^{15}N]lysine bR at a temperature of 200 K. (a) bR_{600}, $\omega_r/2\pi$ = 2.2 kHz, pH 7; (b) bR_{600}, $\omega_r/2\pi$ = 3.0 kHz, pH 2; (c) bR_{560}, $\omega_r/2\pi$ = 3.0 kHz, pH 7; (d) bR_{565}, $\omega_r/2\pi$ = 2.7 kHz, pH 0. The dashed lines indicate the positions of the bR protonated Schiff base nitrogen resonances in the spectra. The difference in isotropic shift between the two purple forms, on the one hand, and the two blue forms, on the other hand, is ~16 ppm.

to generate simulations of MAS spectra that were fit to the experimental data, using the CERN (Geneva) MINUIT fitting package. All calculations were done on microVAX-II computers.

Results

Nitrogen-15 NMR of the Schiff Base Nitrogen. Figure 2 shows the ^{15}N NMR spectra for the various forms of [ϵ-^{15}N]lysine bR. The narrow line at ~8 ppm is from the six ^{15}N-labeled lysine residues in bR that are not involved in the Schiff base linkage, while the line at ~94 ppm is due to the natural-abundance ^{15}N in the peptide backbone. Note that this line is shifted a few ppm upfield in bR_{565}, relative to bR_{560} and bR_{600}. This indicates that in bR_{565}, the pH is sufficiently low to affect the peptide hydrogen bonds. The small doublet at ~146 ppm in Figure 2c comprises the resonances from the bR_{555} and bR_{568} Schiff bases, respectively. This signal appears to be shifted ~16 ppm upfield (to ~130 ppm) in both the deionized and acid blue membrane (Figure 2a,b). In bR_{565}, the all-trans form of the chromophore dominates (Smith & Mathies, 1985; Massig et al., 1985), and the ^{15}N resonance becomes a singlet, centered at 147.6 ppm (Figure 2d). The isotropic shifts for the Schiff base resonances in bR_{560}, bR_{565}, and bR_{600} are listed in Table I.

Carbon-13 NMR Difference Spectroscopy of the Retinal Polyene Chain. Figure 3 presents several ^{13}C MAS NMR spectra for ^{13}C-14 bR. Figure 3a,b contains spectra of the deionized blue species (bR_{600}) obtained at a spinning speed $\omega_r/2\pi$ = 3 kHz. By comparison of these spectra with a spectrum of an unlabeled sample (not shown), the contributions from the label can be identified. The centerbands of these components are indicated with arrows. Close inspection of the downfield resonance (at 121 ppm) reveals a small but

Table I: Comparison of Isotropic Chemical Shifts for the Components in the Solid-State Spectra of Blue Membrane (bR_{600}), Purple Membrane (bR_{555} and bR_{568}), Acid Purple Membrane (bR_{565}), and Retinylidene-*N*-butylimmonium Chloride (PSB)[a]

label	bR_{600}	bR_{555}, 13-cis, 15-syn	bR_{568}, all-trans	PSB model		bR_{565}, all-trans
				6-s-cis, 13-cis	6-s-cis	
[ε-^{15}N]Lys	134.4, 127.3	150.6[f]	143.5[f]		171.7[d]	147.6
^{13}C-15	162.4[g]	163.0	160.1	165.5[c]	167.0[b]	159.3
^{13}C-14	109.2, 110.4, 119.9, 122.4	110.7	122.4	118.2[c]	122.5[b]	119.7
^{13}C-13	169.0	168.7[e]	164.8[e]	162.2[c]	161.8[b]	
^{13}C-12	123.9, 133.5	124.2[c]	134.3[c]	125.1[c]	135.0[b]	
^{13}C-5	148.8	144.1	144.1	131.8[c]	128.7[b]	

[a] All ^{13}C shifts are in ppm relative to external tetramethylsilane (TMS). ^{15}N shifts are in ppm relative to external 5.6 M $^{15}NH_4Cl$. Estimated errors are ±0.2 ppm and are determined by the accuracy of the calibration. [b] Data from Harbison et al. (1985a). [c] Data from Smith et al. (1989). [d] Data from Harbison et al. (1983). [e] Data from Harbison et al. (1985b). [f] Data from de Groot et al. (1988). [g] Average of the isotropic shifts for the two components.

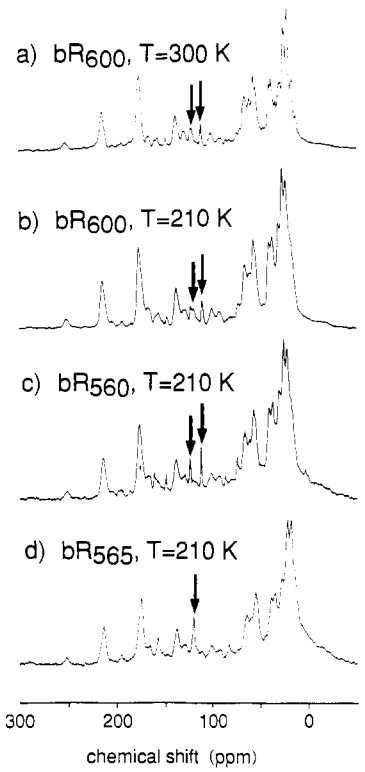

FIGURE 3: Proton-decoupled ^{13}C MAS spectra for ^{13}C-14-labeled blue (bR_{600}) and purple (bR_{560}, bR_{565}) membrane at various temperatures and at a spinning speed $\omega_r/2\pi$ = 3.000 (±0.005) kHz. (a) Deionized blue at ambient temperature; (b) deionized blue at low temperature; (c) neutral purple at low temperature; (d) acid purple at low temperature. In each spectrum, the centerbands of the contributions from the label are indicated by arrows.

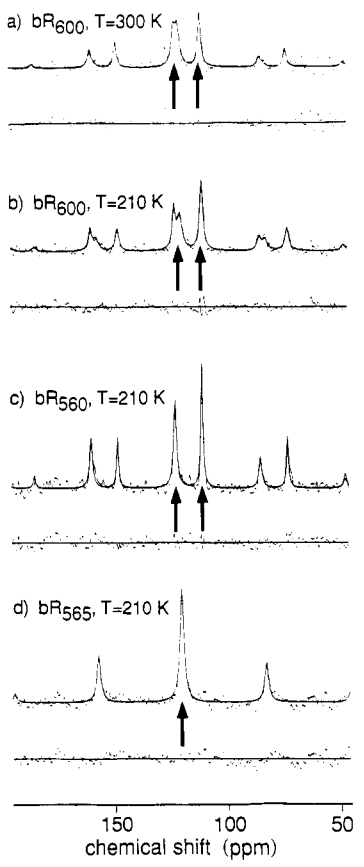

FIGURE 4: Difference spectra for ^{13}C-14-labeled bR_{600}, bR_{560}, and bR_{565} obtained from the spectra in Figure 3 by subtracting a natural-abundance bR_{560} spectrum, taken at the same spinning speed. (a) bR_{600} at ambient temperature and (b) bR_{600}, (c) bR_{560}, and (d) bR_{565} at low temperature. The irregular lines represent the experimental data and the smooth lines the least-squares fits of the data with simulated MAS spectra. Below each difference spectrum the difference between the experimental data and the simulation is shown. Centerbands are indicated by arrows.

significant splitting of approximately 2 ppm.

As has been shown recently, it is very useful to employ difference techniques when the signal from a label is overlapped with a large natural-abundance background signal (de Groot et al., 1988). By subtracting the spectrum of an unlabeled sample taken at exactly the same spinning speed and temperature, it is possible to obtain the high-resolution spectrum of the label alone. Although subtraction decreases the signal to noise ratio, it nevertheless enables a more accurate determination of the principal values of the chemical shift tensor(s), particularly when there is overlap between peaks in the spectrum. It should be noted that subtraction of a natural-abundance bR_{600} spectrum from a natural-abundance bR_{560} spectrum yields only the noise background. Therefore, natural-abundance bR_{560} spectra were used for all subtractions in this work.

Figure 4 shows the difference spectra corresponding to the spectra in Figure 3, and Figure 5 shows low-temperature (170 K < T < 210 K) difference spectra for deionized bR_{600} samples, labeled at various positions along the chromophore. The isotropic shifts for the various resonances are listed in Table I, while Table II contains the principal values of the chemical shift tensors for ^{13}C-5, ^{13}C-12, ^{13}C-14, and ^{13}C-15. (Unfortunately, the signal to noise ratio for the ^{13}C-13 label was too low to obtain the principal values of the chemical shift tensor.)

Low-Temperature Effects. It is important to consider in some detail the effects of lower temperature on the NMR spectra of bR. For example, in comparing Figure 3a and Figure 3b, we discern an overall line broadening with decreasing temperature, in addition to minor changes in line positions. Furthermore, intensity changes are observed in the upfield (aliphatic) region, while the downfield portion of the spectrum remains essentially unchanged. For our purposes,

Table II: Principal Values of the Chemical Shift Tensors (σ_{11}, σ_{22}, and σ_{33}) and Isotropic Shifts (σ_i) for [^{13}C]Retinal-Labeled bR at Low Temperatures (170–200 K)[a]

position	species	σ_{11}	σ_{22}	σ_{33}	σ_i
C-15	bR_{600}	56 (5)	175 (4)	257 (5)	162.4
	bR_{568}	76 (5)	170 (3)	236 (5)	160.1
	bR_{555}	47 (4)	193 (3)	250 (5)	163.0
	bR_{565}	58 (6)	176 (5)	244 (5)	159.3
C-14	bR_{600}, 15-anti[b]	46 (5)	132 (4)	186 (5)	121.1
	bR_{600}, 15-syn[c]	43 (6)	110 (8)	177 (6)	109.8
	bR_{568}, 15-anti	50 (5)	134 (3)	182 (5)	122.4
	bR_{555}, 15-syn	45 (4)	107 (3)	179 (5)	110.7
	bR_{565}, 15-anti	45 (3)	128 (5)	185 (3)	119.7
C-12	bR_{600}, 13-trans	58 (4)	141 (4)	202 (4)	133.5
	bR_{600}, 13-cis	37 (5)	138 (5)	197 (4)	123.9
	bR_{568},[d] 13-trans	58 (6)	135 (8)	210 (6)	134.3
	bR_{555},[d] 13-cis	35 (5)	132 (7)	206 (5)	124.2
C-5	bR_{600}	29 (4)	174 (3)	244 (4)	148.8
	bR_{560}	28 (3)	170 (2)	236 (5)	144.1

[a] Shifts are in ppm relative to external TMS. The errors (±) for the tensor elements are given in parentheses. They represent a 95% confidence interval and are statistically determined. The errors for the isotropic shifts are determined by the accuracy of the calibration and are estimated as ±0.2 ppm. [b] Average of components A and B. [c] Average of components C and D. [d] Data from Smith et al. (1989).

the important point is that the [^{13}C]retinal centerbands, indicated by the arrows, are not significantly affected. The results for the ^{13}C-14 resonance are summarized in Table III. For bR_{560}, the variations are quite small (<0.3 ppm) and of the same magnitude as the experimental errors, while the effects in bR_{600} are slightly larger. For the other ^{13}C labels, we also found that the variations of the isotropic chemical shifts with temperature were always only a fraction of a ppm. Furthermore, the principal values of the chemical shift tensors were temperature-independent within experimental error. This justifies the use of the low-temperature difference techniques in order to study the variation of the opsin shift with deionization and acidification.

Assignments. For ^{13}C-12, ^{13}C-14, ^{13}C-15, and [ϵ-^{15}N]Lys bR_{600}, the label contributes a doublet to the spectrum.

For C-14 the γ effect (a strong steric interaction) in the 15-syn form requires that its C-14 resonance is upfield from that in the 15-anti form (Harbison et al., 1984). Therefore, the assignment of the C-14 15-anti and 15-syn signals in bR_{600} should be the same as for bR_{560} (Harbison et al., 1984, 1985; Smith et al., 1989).

In the ^{13}C-12 bR_{600} spectrum, the difference in the isotropic chemical shift for the two components is equal to that found for bR_{560} (~10 ppm) and is similarly localized in the σ_{11} shift tensor element. This is consistent with a γ effect between

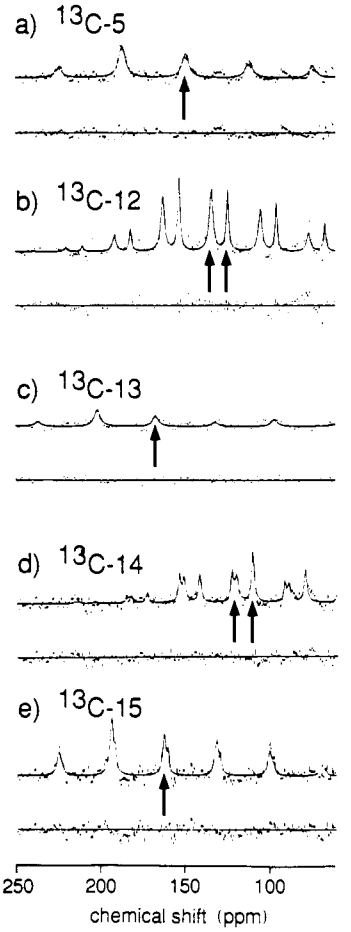

FIGURE 5: Difference spectra for deionized bR_{600} labeled at various positions in the conjugated chain of the chromophore. (a) ^{13}C-5, $\omega_r/2\pi$ = 3.0 kHz, T = 180 K; (b) ^{13}C-12, $\omega_r/2\pi$ = 2.3 kHz, T = 230 K; (c) ^{13}C-13, $\omega_r/2\pi$ = 2.8 kHz, T = 200 K; (d) ^{13}C-14, $\omega_r/2\pi$ = 2.5 kHz, T = 170 K; (e) ^{13}C-15, $\omega_r/2\pi$ = 2.5 kHz, T = 170 K. The irregular lines represent the experimental data and the smooth lines the least-squares fitted simulations. Below each spectrum the difference between the experimental data and the simulation is shown. Centerbands are indicated by arrows.

protons attached to C-12 and C-15 (Harbison et al., 1985). Hence, the downfield signal in the difference spectrum is from the chromophore in the 13-trans form, and the upfield signal is from the 13-cis form. This assignment is in agreement with the isomer ratio found in chemical extraction studies (Mowery et al., 1979; Fisher & Oesterhelt, 1979; Smith & Mathies, 1985; Massig et al., 1985; Scherrer et al., 1989).

For ^{13}C-15, and [ϵ-^{15}N]Lys bR in bR_{600}, an assignment of conformations is not possible at this stage.

Table III: [14-^{13}C]Retinal Isotropic Chemical Shifts (σ_i), Line Widths (FWHM), and Fractions (f) of the Four Components (A–D) in the Deionized Blue Membrane (bR_{600}) Spectra (See Figure 6), the Two Components (bR_{568} and bR_{555}) in the Dark-Adapted PM (bR_{560}) Spectra, and the Single Component in the Acid Purple (bR_{565}) Spectra[a]

		ambient temperature			low temperature		
species	conformation	σ_i (ppm)	FWHM (ppm)	f (%)	σ_i (ppm)	FWHM (ppm)	f (%)
bR_{600}(A)	15-anti	122.1 (0.3)	1.4 (0.7)	28 (10)	122.4 (0.3)	1.4 (0.5)	24 (5)
bR_{600}(B)	15-anti	120.4 (0.3)	2.4 (0.7)	28 (9)	119.9 (0.4)	2.5 (0.5)	31 (5)
bR_{600}(C)	15-syn	110.4 (0.3)	1.4 (0.3)		110.4 (0.2)	0.9 (0.3)	34 (3)
bR_{600}(D)	15-syn	110.4 (0.3)	1.4 (0.3)		109. 2 (0.2)	0.9 (0.3)	11 (3)
bR_{568}	15-anti	122.0 (0.2)[b]	1.4 (0.2)	48 (3)	121.7 (0.2)	0.7 (0.2)	44 (3)
bR_{555}	15-syn	110.5 (0.2)[b]	0.9 (0.2)	52 (3)	110.2 (0.2)	0.7 (0.2)	56 (3)
bR_{565}	15-anti				119.7 (0.3)	2.4 (0.4)	
PSB	15-anti	122.5 (0.2)					
PSB	15-syn	118.2 (0.2)					

[a] Isotropic chemical shifts (σ_i) are in ppm relative to external TMS. Estimated errors for σ_i (±) are determined by the accuracy of the calibration. The errors for the line widths and the fractions (±) are statistically determined and represent a 95% confidence interval. [b] Data from de Groot et al. (1988).

Discussion

Deionization or acidification of bR has a pronounced effect on the visible absorption spectrum of the pigment. The origin of the observed color changes may be variations in hydrogen bonding at the Schiff base, or concentration-dependent conformational changes of the retinal and/or protein. Changes in hydrogen bonding at the Schiff base should appear predominantly in the ^{15}N NMR spectrum because it is known that the ^{15}N chemical shift in protonated retinal Schiff bases depends strongly on the nature of the counterion (Harbison et al., 1983; de Groot et al., 1989) and that the effect tapers off rapidly with distance along the polyene chain (Harbison et al., 1985b). Conformational changes, on the other hand, may be expected to influence the chromophore locally, wherever they occur, and may appear in the ^{13}C spectra as line broadening, splitting, or chemical shift changes. We shall discuss these effects separately.

Mechanism of the Purple to Blue to Purple Transitions and the Complex Counterion Model. Among the sites studied thus far, the only change in chemical shift which correlates entirely with the variation of the opsin shift in the purple to blue to purple transitions is the ~16 ppm change at the Schiff base nitrogen, which is also by far the largest shift difference observed among theses species. It has been shown previously that the ^{15}N chemical shift tensor of protonated Schiff bases is extremely sensitive to variations in counterion properties (Harbison et al., 1983; de Groot et al., 1988). Mutual polarization of the chromophore and the counterion affects the distribution of the π electrons over the conjugated system, the effect being the strongest at the Schiff base nitrogen (Harbison et al., 1985b). This behavior has been thoroughly characterized for all-trans PSB model compounds with widely different counterions (de Groot et al., 1989). Over a series of simple halide, phenolate, and carboxylate counterions, it was found that (i) the isotropic chemical shift varies between 155 and 175 ppm, (ii) σ_{11} is almost constant (19 ppm $< \sigma_{11} <$ 27 ppm), and (iii) there is a strong linear correlation between σ_{22} and σ_{33}. Interestingly, bR_{568} shows the same relationship between σ_{22} and σ_{33}, with σ_{11} = 14 (±8), in the same range as the model compounds. However, the isotropic shift (143.5 ppm) is far upfield of the PSB models, suggesting an extremely weak hydrogen bond in bR.

In the two forms of bR_{600}, the ^{15}N Schiff base resonances are shifted upfield by an additional ~16 ppm relative to bR_{568}. Thus, bR_{600} is even further outside the range of the model compounds[3] than bR_{568}. This suggests that the "counterion strength" [as defined by de Groot et al. (1989)] is still weaker than in bR_{568} and makes it even less likely that the counterion comprises a single amino acid residue, such as a tyrosinate or aspartate. Therefore, the present ^{15}N data provide additional support for the complex counterion model invoked in the previous work (de Groot et al., 1989).

Several possible mechanisms have been proposed for the purple to blue to purple transition: (i) protonation of the Schiff base counterion followed by binding of an anion at the same site to restore the purple color (Fischer & Oesterhelt, 1979; Massig et al., 1985); (ii) protonation of the Schiff base counterion followed by protonation of a second group near the ionone ring to restore the purple color (Mowery et al., 1979); and (iii) a sequence of two distortions of the protein between two conformations, so that in the acid purple form the original bR_{570} conformation is more or less restored (Szundi & Stoeckenius, 1987). In its simplest form, the first proposal would amount to replacing the counterion by a simple chloride anion. However, in that case, an isotropic shift for bR_{565} around 172 ppm is expected (Harbison et al., 1983), and this contradicts the experimental findings (148 ppm). The second proposal would imply that the ^{15}N isotropic shifts of bR_{565} and bR_{600} would be roughly equal, whereas we find a 16 ppm difference. Finally, the third proposal does not address the specific effects observed at the Schiff base. Furthermore, the evidence which we observe for conformational distortions correlates with the variation of pH, and not with the changes in λ_{max} (see below). Hence, the blue to acid purple transition is not simply a restoration of the original retinal configuration. On the contrary, the ^{13}C results suggest that the chromophore distortions progress, rather than reverse, upon further acidification (see below).

The experimental data can be reconciled with a mechanism that extends (i) to incorporate the idea of a complex counterion recently discussed by de Groot et al. (1989)—i.e., we interpret

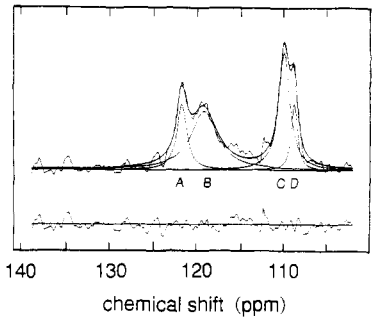

FIGURE 6: Centerband region of one of the 0.3 ppm/point, low-temperature difference spectra taken for ^{13}C-14 deionized bR_{600} at $\omega_r/2\pi$ = 3.000 (±0.005) kHz (thin irregular line), together with the least-squares fitted simulation (thick smooth line) and the residue (below). The various components that constitute the fit are also shown (thinner smooth lines) and are denoted A–D. A and B are due to the 15-anti form of bR_{600} while C and D are due to the 15-syn form.

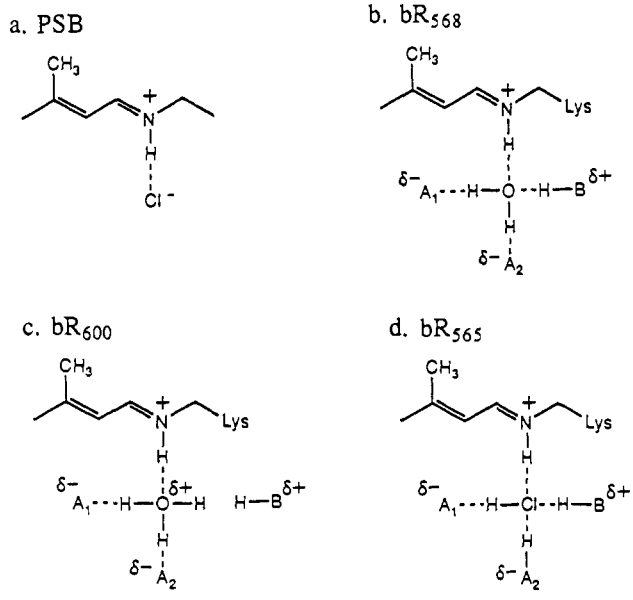

FIGURE 7: Schematic representation of the complex counterion model and the purple to blue to purple transitions. (a) Protonated Schiff base model compound, single counterion. (b) A complex counterion for bR_{560}. (c) Corresponding complex counterion for bR_{600}, containing an extra proton. (d) Corresponding complex counterion for bR_{565}, like bR_{560}, but with the water molecule replaced by HCl.

[3] Unfortunately, the peaks are too broad to collect a spectrum at the very low spinning speed necessary to accurately determined the principal components of the shielding tensor. However, the experimental observation that there are only very weak sidebands for the Schiff base resonances in the spectrum for deionized bR_{600} (Figure 2a, $\omega_r/2\pi$ = 2.2 kHz) shows that the shift antisotropy is very small, as expected from the trend found in the earlier work.

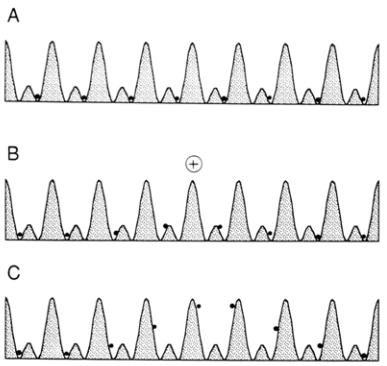

FIGURE 8: Schematic representation of autolocalized topological excitations in an H-bonded chain. (A) Ground state. (B) Negative ionic effect. (C) Bjerrum D defect.

the purple to blue transition as the protonation of the complex counterion. By a complex counterion, we mean a strongly hydrogen bonded network, consisting of several protic species. In the example represented schematically in Figure 7b–d, a water molecule is supported by four hydrogen bonds, one with the Schiff base, two with proton donors (A_1H and A_2H), and one with another proton acceptor (B), in order to obtain the correct stoichiometry. This type of structure has recently been considered theoretically in connection with proton conduction in ice (Antonchenko et al., 1983; Pnevmatikos, 1988) and experimentally, in ammonium nitrate complexes (Einstein & Tuch, 1970). The extended network of hydrogen bonds results in charge delocalization. For phenolic protons in intramolecular hydrogen-bonded structures, it has been experimentally verified that the polarizability increases with the number of hydrogen bonds (Brzezinski et al., 1987) in agreement with these ideas.

The relevant properties of such systems are illustrated in Figure 8 for the simplest case of a one-dimensional, strongly hydrogen-bonded network (an H-bonded chain). The series of double-well potentials represents the potential energy for a single proton along the line connecting the heavy atoms that form the H-bonded chain. When several protons populate the chain, the electrostatic repulsions between them make a further contribution to the energy which depends on their spacing. Figure 8A shows one of the doubly degenerate ground states of the chain.

The proton system can be disturbed in two ways. In Figure 8B, an external positive charge induces a negative ionic (I^-) defect. The protons are redistributed over several bonds because of their mutual repulsion. Thus, the H-bonded chain forms a soft, diffuse counterion to the external charge. The proton system can also be disturbed by changes in the proton chemical potential of the environment so that the chain is either deprotonated (e.g., at high pH) or protonated (e.g., at low pH). In Figure 8C, an extra proton generates a Bjerrum D (Doppelt) defect. Such a defect is created when the proton chemical potential exceeds the defect creation energy. Again, the protons are redistributed over several bonds due to their mutual repulsion, and the result is delocalization of the positive charge of the added proton. A careful theoretical study of these phenomena suggests a defect size of a few bond lengths, with a creation energy considerably lower than the energy that would be required to (de)protonate an individual site in the chain (Tsironis & Pnevmatikos, 1989). Furthermore, defects move relatively freely along the chain, with low energy barriers. Analogous arguments hold equally well for H-bonded networks of higher dimensions.

Figure 7b shows the state of the putative counterion complex in bR_{560}. The protonated Schiff base induces a negative ionic defect in the H-bonded network. The result is an exceedingly soft and diffuse counterion compared to the halide in Figure 7a. Figure 7c shows the corresponding counterion for bR_{600}. An extra proton, accommodated in a Bjerrum defect, further reduces the counterion strength. This defect will occur abruptly when the proton chemical potential exceeds the defect creation energy. Furthermore, since the defect creation energy depends on the strength of the H bonds in the complex, which in turn depend on structural distortions, variation of either the membrane potential or the pH can cause an abrupt transition from purple to blue, in agreement with experimental observations (Chronister et al., 1986). The other transition, from blue to acid purple, may be explained by exchanging an OH^- for a Cl^-, as shown in Figure 7d. The quintessence is that both a chloride and an oxygen may support four hydrogen bonds in a network. However, an OH^- includes a proton, whereas a Cl^- does not. Therefore, exchange of an OH^- by a Cl^- creates a proton deficit or Bjerrum L (Leer) defect in the counterion that can serve to annihilate the D defect in the blue species, and approximately restore the situation that was observed in bR_{560}.

Four additional remarks are in order. First, it may be noted that this model also supports the resonance Raman results (Smith & Mathies, 1985; Massig et al., 1985) that indicated reversibility similar to that observed in the ^{15}N NMR. Second, Fischer and Oesterhelt (1979) have shown that various halides in high concentration induce the blue to acid purple transition, but in each case with different λ_{max}. Their experiments suggest a direct interaction between the Schiff base and the halide in the acid purple form. Within the context of our model, this would mean that the water molecule, which we have depicted in Figure 7b as being directly involved in the Schiff base hydrogen bond, is replaced by HCl in bR_{565} (see Figure 7d). Third, there is direct NMR evidence for rapid exchange of the Schiff base proton with bulk water (Harbison et al., 1988). The extended multidimensional hydrogen-bonding system of the proposed complex counterion provides a path for such exchange to take place. Fourth, hydrogen-bonded complex anions can also be formed in solution by the homoconjugation of organic acids in nonprotic solvents (Kolthoff et al., 1966). These complex anions are thought to explain the exceptionally large red shifts of retinal Schiff bases in such solutions (Sheves et al., 1983).

Some additional insight into hydrogen-bonding effects may be gained by estimating the amount of negative charge involved in the polarization effects at the nitrogen. Here, we compare the ^{15}N shifts for bR_{565}, bR_{560}, bR_{600}, and the protonated Schiff base salt *all-trans*-retinylidene-*N*-butyl[^{15}N]ammonium chloride. The ^{15}N isotropic chemical shift of the latter (172 ppm) was measured by Harbison et al. (1983). Using a (conservative) conversion factor of 150–300 ppm per electron (Harbison et al., 1983), we estimate the variation of the nitrogen charge in the purple to blue to purple transition to be 0.05–0.1 electronic equiv, while the difference between the chloride model compound and bR_{560} is estimated as 0.08–0.16 electronic equiv.

The latter difference is attributed to the hydrogen bonding in the complex counterion (Figure 7b), which is absent in the PSB salt (Figure 7a). Presumably, the charge differences at the counterion atom directly hydrogen bonded to the Schiff base nitrogen should be considerably larger than 0.08–0.16 electronic equiv to account for the polarizability of the polyene system. Hydrogen-bond charge transfers are usually a little under 0.1 electronic equiv (Hofacker, 1983). Therefore, if the counterion atom is stabilized by three hydrogen bonds, a total

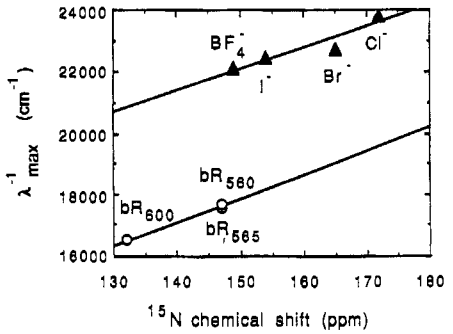

FIGURE 9: Inverse of λ_{max} in the solid state plotted against the ^{15}N isotropic chemical shift, for the three bR species—bR_{568}, bR_{565}, and bR_{600}—which contain all-trans chromophores (O), and for the Cl^-, Br^-, and I^- salts of retinylidene-*N*-butylamine which have 6-s-cis conformations (▲). The solid lines represent linear least-squares fits through the data points.

charge transfer up to 0.3 electron charge equiv may be considered as reasonable, which is of the correct order of magnitude.

The variation of 0.05–0.10 electronic equiv in the ^{15}N electron density between bR_{600} and bR_{568} or bR_{565} is almost as large as the difference between the PSB salt and bR_{568} or bR_{565}. Thus, it is unlikely that a subtle change in the character of the counterion (i.e., small changes in hydrogen-bonding properties) could account for the difference between PM and blue membrane. In order to explain the large upfield shift of the ^{15}N resonance in bR_{600}, an additional strong mechanism is needed. Protonation of the complex counterion involves the addition of a full positive charge to the counterion. Considering that the delocalization of the positive charge should be ~2 O–O distances (Antonchenko et al., 1983; Pnevmatikos et al., 1988), the defect could be centered in any of the three hydrogen bonds that surround the water molecule. Figure 7c shows a possible structure for the protonated complex with the hydrogen-bonding defect tentatively located in the hydrogen bond with the proton–acceptor.

Contribution of Schiff Base Hydrogen Bond Strength to the Opsin Shift. Although it has been qualitatively demonstrated that the Schiff base hydrogen bond in the various bR species is very weak, the size of the contribution of this interaction to the total opsin shift of 5100 cm^{-1} has not been determined. This is because the relation between local parameters, such as stretching frequencies or NMR chemical shifts, and nonlocal parameters, such as the λ_{max}, is not well established. However, by comparing the relationship between λ_{max} and the experimental ^{15}N chemical shift for the various forms of bR reported here, as well as with the corresponding data for some PSB model compounds, a reasonable estimate can be given for the fraction of the opsin shift associated with differences in hydrogen-bonding strength.

In Figure 9, the inverse of λ_{max} is plotted against the ^{15}N isotropic chemical shift, for bR_{565}, bR_{600}, and bR_{568}, and for the Cl^-, Br^-, and I^- salts of *N-all-trans*-retinylidenebutylamine. These data are for PSB models *in the solid state*, and introduce the "solid state opsin shift", which we define as the difference in excitation energy between the all-trans chloride salt and bR_{568} (~6000 cm^{-1}). Interestingly, this shift is larger than the solution opsin shift (~5100 cm^{-1}), based on the all-trans chloride PSB in an aprotic solvent. The solid lines in Figure 8 are based on linear least-squares fits through the data points, and the slope, $\partial\lambda_{max}/\partial\sigma_i \sim 70$ cm^{-1} ppm, is roughly the same in both cases, which suggests the similarity of the mutual polarization mechanism for the Schiff base in the PSB model compounds and in bR. The measured values for the ^{15}N shifts in the *n*-butylretinal hydrochloride (a strongly hydrogen-bonded PSB) and bR_{568} (the all-trans component) are 171.7 and 143.5 ppm, respectively. Thus, the contribution of the weak hydrogen bonding to the opsin shift is ~2000 cm^{-1}.

The remainder of the opsin shift (~3100 cm^{-1}) has been attributed to 6-s-cis → 6-s-trans isomerization and to perturbations induced by the protein. An estimate of the size of the contribution from 6-s isomerization has emerged from studies of retinal analogues which are locked in the 6-s-cis or 6-s-trans conformations, specifically, 8,16-methanoretinals (van der Steen et al., 1986). In this case, it appears that ~1200 cm^{-1} can be attributed to the isomerization, thus leaving 1900 cm^{-1} to be ascribed to the protein perturbations. However, other evidence suggests that the contribution of the 6-s-cis to *trans*-retinal isomerization may be considerably larger. Sheves and co-workers (Albeck et al., to be published) have found that a weakly H-bonded all-trans PSB formed from 1,1-didemethylretinal shows a λ_{max} = 550 nm and a ^{13}C-5 chemical shift of 144 ppm, values which are comparable to those observed in bR. These results indicate that the simple combination of 6-s isomerization and weak H bonding can yield very large red shifts, sufficient to fully explain the opsin shift in bR.

Blue Membrane Is a Mixture of at Least Four Different Species. Resonance Raman spectroscopy (Smith & Mathies, 1985; Massig et al., 1985; Pande et al., 1985) and chemical extraction experiments (Mowery et al., 1979; Pande et al., 1985) suggested that the blue membrane contains a mixture of 13-*cis*- and 13-*trans*-retinylidene chromophores, as does dark-adapted PM. This is in agreement with the present ^{13}C-12 NMR results which show a 13-trans:13-cis ratio of 11:9 in blue membrane. Our ^{13}C-14 NMR results also show a 15-anti:15-syn ratio of 11:9. This suggests that the chromophores in blue membrane are all 13-cis,15-syn or 13-trans,15-anti as in bR_{560}. However, the ^{13}C-14 results show that, unlike bR_{560}, the blue membrane contains two different forms of the 15-syn chromophore and two different forms of the 15-anti chromophore. The difference spectra in Figure 4 show a splitting in the 15-anti component that increases somewhat at lower temperatures. The spectra in Figures 4a,b were fitted with a superposition of three MAS patterns. Inspection of the residue (in each case plotted below the spectrum) shows an irregularity in the fit of the 15-syn peak for the low-temperature spectrum (Figure 4b), which is absent in the room temperature spectrum (Figure 4a), and suggests a small splitting for the 15-syn peak in the low-temperature spectrum as well. In Figure 6, the centerband region of ^{13}C-14 bR_{600} is shown, taken with a resolution of ~0.3 ppm per point before zero-filling, and a minor splitting of the 15-syn peak is clearly observed. The residue after fitting the spectrum with a superposition of four components, denoted A–D, contains only noise.

Components A and C together represent a substantial part of the total intensity in the bR_{600} difference spectrum (~58%) and show a remarkable resemblance to the two components of the low-temperature spectrum of bR_{560} (i.e., the 15-*anti*-bR_{568} and the 15-*syn*-bR_{555}, respectively). Not only are the ^{13}C-14 isotropic shifts and line widths similar but also the principal values of the shift tensor appear to be the same within experimental error (Table II). These data suggest that, for about half of the bR_{600} chromophores, environmental influences at the 14 position are very similar to those in bR_{560}. The difference spectra for ^{13}C-15 recorded with the higher digital resolution of 0.3 ppm/point provide additional support for these inferences. There is conclusive evidence for a narrow shoulder

on the upfield side of the resonance in bR_{600} (cf. Figure 5e). The shoulder represents a significant part of the spectral intensity in the difference spectrum (>10%), and the isotropic shift (159.8 ppm) is very close to that of the all-trans component of bR_{560} (160.1 ppm).

We would like to emphasize that the NMR experiments on ^{13}C-14 bR_{600} and ^{13}C-15 bR_{600} were repeated several times, and in the case of the ^{13}C-14 position on two different samples, with essentially the same results. In one case, the sample was dialyzed, packed in a rotor, and subsequently dialyzed another time, in order to ensure that the purple to blue transition was complete. Moreover, the peculiar purple-type components were not observed in the bR_{600} spectra of the ^{13}C-5, ^{13}C-12, and [ϵ-^{15}N]lysine samples that were prepared according to the simple dialysis procedures described under Materials and Methods, so we have no reason to believe that dialysis would not yield a completely blue bR_{600} sample. Hence, we conclude that bR_{600} is a mixture of at least four different species.

Figures 3d and 4d also contain a ^{13}C-14 spectrum for the acid purple bR (bR_{565}). In this case, the label yields a single signal, which is due to the chromophore in the 15-anti configuration. This is consistent with resonance Raman results (Smith & Mathies, 1985; Massig et al., 1985). The analysis of the NMR difference spectrum reveals that, within experimental error, the bR_{565} signal has the same isotropic shift and also the same principal values of σ as component B in the ^{13}C-14 blue spectra. In addition, data for an acid purple ^{13}C-15 sample are listed in Table II. Consistent with our observations at the 14 position, the acid purple form yields only one signal, and the shoulder that was present in the blue signal has disappeared in the acid purple bR. Interestingly, the values for the principal components of σ are in between those for the two components of bR_{560} (cf. Table II).

For the blue ^{13}C-14 samples, the intensity ratio, as determined with NMR, between 15-anti and 15-syn is 11:9, whereas in bR_{560} it is approximately the opposite, 9:11. Compare now the bR_{600} spectrum with the one in Figure 4d which is for bR_{565}. The latter contains only one component, which is spectroscopically identical with component B in the bR_{600} spectrum. Thus, it appears that the relative amount of 15-*anti*-bR increases with decreasing pH, until at pH 0 there is only 15-anti present. Furthermore, in going from neutral pH to pH 0, the relative intensity of the A and C components decreases, while the amount of B increases. The color, however, changes from purple to blue at pH 2, and back to purple at pH 0. Therefore, the variation of the relative amounts of the four components in bR_{600} does not correlate with the variation of the opsin shift.

Line Broadening in the Spectra of Blue and Acid Purple Membrane. The lines from the labels are much broader in bR_{600} than in bR_{560}. For instance, compare the spectra of ^{13}C-14 bR in Figure 3a and Figure 3b (and also in Figure 4a and Figure 4b) with the one in Figure 3c (and Figure 4c). The same holds true for the other labels. The bR_{600} difference spectra of Figure 5 all show features that are much broader than what has been found in the corresponding bR_{560} (difference) spectra (Harbison et al., 1985; Smith et al., 1989). The ^{13}C-5 bR_{600} spectra show one broad component (FWHM ~4 ppm) shifted downfield by ~4 ppm from the corresponding resonance in bR_{560}. Apart from some additional line broadening (FWHM ~2.4 ppm and FWHM ~1.4 ppm for the 13-trans and 13-cis component, respectively), the spectrum for ^{13}C-12 bR_{600} is very similar to what has been observed for bR_{560} (Harbison et al., 1985; Smith et al., 1989). The 13-trans peaks are upfield-shifted by only 0.7 ppm, and the 13-cis peaks by only 0.3 ppm. For the ^{13}C-13 and the ^{13}C-15 bR_{600}, again only one broad feature is observed.

The broad lines in all the NMR spectra of blue and acid purple bR indicate irregular conformational changes in both species. These presumably arise from the increase in membrane potential associated with the proton exchange at the low-affinity cation binding sites, which are thought to be located on the membrane surface (Szundi & Stoeckenius, 1987). The exchange at the low-affinity sites probably disturbs the membrane structure, and therefore the bR_{600} molecules embedded in it. Conformational distortions were indicated previously by X-ray diffraction (Kimura et al., 1984; Heyn et al., private communication), circular dichroism (Kimura et al., 1984), and resonance Raman spectroscopy (Smith & Mathies, 1985; Massig et al., 1985).

Effects of the Neutral Purple to Blue Transition at the Ionone Ring. The ^{13}C resonance of the 5 position is shifted by 4.7 ppm downfield in bR_{600} relative to bR_{560} This change in isotropic shift is consistent with findings that environmentally induced changes in the C-5 chemical shift and the λ_{max} of an all-trans PSB in solution are correlated with a slope of ~2 ppm/25 nm (Albeck et al., to be published). We are in the process of studying these all-trans PSB model compounds in the solid state to determine which chemical shift tensor elements are involved in the effect. Such data may permit an interpretation of the C-5 shift tensor elements in Table II. We are also studying the C-5 resonance in acid purple bR to see whether it follows color rather than pH (in contrast to the pattern of the weaker changes seen in the other carbon chemical shifts).

Conclusions

A detailed study of the mechanism of the opsin shift in bR has been performed via the investigation of the several species that occur as a result of deionization and acidification. Several conclusions can be drawn: (i) The effects on the opsin shift occur primarily through changes in the Schiff base H bond. Although we cannot state that this is the *only* mechanism, the extent of the effect does not seem to leave much room for alternatives. However, it may be of interest to investigate the behavior of the C-5 chemical shifts upon acidification to pH 0. (ii) The data provide further support for the complex counterion model. None of the other available models for the mechanism of the purple to blue to purple transitions yields a satisfactory explanation of the present findings. (iii) An estimate of 2000 cm^{-1} was obtained for the portion of the opsin shift that is associated with hydrogen-bonding changes at the Schiff base. (iv) Upon lowering the pH, conformational distortions are discernible at C-13, C-14, and C-15. (v) There is evidence that the blue membrane contains at least four different species.

Acknowledgments

P. B. Rosenthal is gratefully acknowledged for providing the solid-state spectroscopic data for the halide PSB model compounds.

Registry No. *all-trans*-Retinal, 116-31-4; 13-*cis*-retinal, 472-86-6; *all-trans*-retinylidene-*N*-butylammonium chloride, 61769-46-8; 13-*cis*-retinylidene-*N*-butylammonium chloride, 127064-66-8.

References

Andrew, A. R., Bradbury, A., & Eades, R. G. (1958) *Nature (London) 182*, 1659.

Antonchenko, V. Ya., Davydov, A. S., & Zolotariuk, A. V. (1983) *Phys. Status Solidi B 115*, 631–640.

Argade, P. V., Rothschild, K. J., Kawamoto, A. H., Herzfeld, J., & Herlihy, W. C. (1981) *Proc. Natl. Acad. Sci. U.S.A. 78*, 1643–1646.

Bagley, K., Dollinger, G., Eisenstein, L., Singh, K., & Zimanyl, L. (1982) *Proc. Natl. Acad. Sci. U.S.A. 79*, 4972–4976.

Blatz, P. E., & Mohler, J. H. (1975) *Biochemistry 14*, 2304–2309.

Brzezinski, B., Zundel, G., & Krämer, R. (1987) *J. Phys. Chem. 91*, 3077–3080.

Chang, C.-H., Chen, J.-G., Govindjee, R., & Ebrey, T. G. (1985) *Proc. Natl. Acad. Sci. U.S.A. 82*, 396–400.

Chronister, E. L., Corcoran, T. C., Song, L., & El-Sayed, M. A. (1986) *Proc. Natl. Acad. Sci. U.S.A. 83*, 8580–8584.

Courtin, J. M. L., Lam, G. K., Peters, A. J. M., & Lugtenburg, J. (1985) *Recl. Trav. Chim. Pays-Bas 104*, 284–291.

de Groot, H. J. M., Copiê, V., Smith, S. O., Allen, P. J., Winkel, C., Lugtenburg, J., Herzfeld, J., & Griffin, R. G. (1988) *J. Magn. Reson. 77*, 252–257.

de Groot, H. J. M., Harbison, G. S., Herzfeld, J., & Griffin, R. G. (1989) *Biochemistry, 28*, 3346–3353.

Einstein, F. N. B., & Tuch, D. G. (1970) *Acta Crystallogr. B26*, 1117–1120.

Fischer, U., & Oesterhelt, D. (1979) *Biophys. J. 28*, 211–230.

Griffin, R. G., Aue, W. P., Haberkorn, R. A., Harbison, G. S., Herzfeld, J., Menger, E. M., Munowitz, M. G., Olejniczak, E. T., Raleigh, D. P., Roberts, J. E., Ruben, D. J., Schmidt, A., Smith, S. O., & Vega, S. (1988) in *Physics of NMR Spectroscopy in Biology and Medicine*, Proceedings of the Enrico Fermi International School of Physics, July 8–18, 1986 Varenna, Italy, North-Holland Press, Amsterdam.

Harbison, G. S., Herzfeld, J., & Griffin, R. G. (1983) *Biochemistry 22*, 1–5.

Harbison, G. S., Smith, S. O., Pardoen, J. A., Winkel, C., Lugtenburg, J., Herzfeld, J., Mathies, R., & Griffin, R. G. (1984) *Proc. Natl. Acad. Sci. U.S.A. 81*, 1706–1709.

Harbison, G. S., Smith, S. O., Pardoen, J. A., Courtin, J. M. L., Lugtenburg, J., Herzfeld, J., Mathies, R. A., & Griffin, R. G. (1985a) *Biochemistry 24*, 6955–6962.

Harbison, G. S., Mulder, P. P. J., Pardoen, H., Lugtenburg, J., Herzfeld, J., & Griffin, R. G. (1985b) *J. Am. Chem. Soc. 107*, 4809–4816.

Harbison, G. S., Roberts, J. E., Herzfeld, J., & Griffin, R. G. (1988) *J. Am. Chem. Soc. 110*, 7221–7223.

Henderson, R., & Unwin, P. (1975) *Nature 257*, 28–32.

Herzfeld, J., & Berger, A. E. (1980) *J. Chem. Phys. 73*, 6021–6030.

Hildebrandt, P., & Stockburger, M. (1984) *Biochemistry 23*, 5539–5548.

Hofacker, G. L. (1983) in *Biophysics* (Hoppe, W., Lohmann, W., Markl, H., & Ziegler, H., Eds.) pp 207–263, Springer-Verlag, Berlin.

Honig, B., Greenberg, A. D., Dinur, U., & Ebrey, T. G. (1976) *Biochemistry 15*, 4593–4599.

Khorana, H. G., Gerber, G. E., Herlihy, W. C., Gray, C. P., Anderegg, R. J., Nibei, K., & Biemann, K. (1979) *Proc. Natl. Acad. Sci. U.S.A. 76*, 5046–5050.

Kimura, Y., Ikegami, A., & Stoeckenius, W. (1984) *Photochem. Photobiol. 40*, 641–646.

Kolthoff, I. M., Chantooni, M. K., & Bhowmik, S. (1966) *J. Am. Chem. Soc. 88*, 5430–5439.

Lozier, R. H., Bogomolni, R. A., & Stoeckenius, W. (1975) *Biophys. J. 15*, 955–962.

Lugtenburg, J., Muradin-Szweykowska, M., Heeremans, C., Pardoen, J. A., Harbison, G. S., Herzfeld, J., Griffin, R. G., Smith, S. O., & Mathies, R. A. (1986) *J. Am. Chem. Soc. 108*, 3104–3105.

Maricq, M. M., & Waugh, J. S. (1979) *J. Chem. Phys. 70*, 3300–3316.

Massig, G., Stockburger, M., & Alshut, Th. (1985) *Can. J. Chem. 63*, 2012–2017.

Mathies, R. A., Smith, S. O., Harbison, G. S., Courtin, J. M. L., Herzfeld, J., Griffin, R. G., & Lugtenburg, J. (1986) *Proceedings of the 2nd International Conference on Retinal Proteins*, July 22–25, 1986, Irkutsk, USSR, VNU Science Press, Utrecht, The Netherlands.

Mogi, T., Stern, L. J., Marti, T., Chao, B. H., & Khorana, H. G. (1988) *Proc. Natl. Acad. Sci. U.S.A. 85*, 4148–4152.

Mowery, P. C., Lozier, R. H., Chae, Q., Tseng, Y.-W., Taylor, M., & Stoeckenius, W. (1979) *Biochemistry 18*, 4100–4107.

Muradin-Szweykowska, M., Pardoen, J. A., Dobbelstein, D., van Amsterdam, L. J. P., & Lugtenburg, J. (1984) *Eur. J. Biochem. 140*, 173–176.

Nakanishi, K., Balogh-Nair, V., Arnaboldi, M., Tsujimoto, K., & Honig, B. (1980) *J. Am. Chem. Soc. 102*, 7945–7947.

Oesterhelt, D., & Stoeckenius, W. (1971) *Nature (London), New Biol. 233*, 149–152.

Oesterhelt, D., & Stoeckenius, W. (1973a) *Proc. Natl. Acad. Sci. U.S.A. 70*, 2853–2857.

Oesterhelt, D., & Stoeckenius, W. (1973b) *Methods Enzymol. 31*, 667–678.

Ohtani, H., Kobayashi, T., Iwai, J., & Ikegami, A. (1986) *Biochemistry 25*, 3356–3363.

Oseroff, A. R., & Callender, R. H. (1974) *Biochemistry 13*, 4243–4248.

Ovchinnikov, Yu. A., Abdulaev, N. G., Fergina, M. Yu., Kiselev, A. V., & Lobanov, N. A. (1977) *FEBS Lett. 84*, 1–4.

Ovchinnikov, Yu. A., Abduleaev, N. G., Fergina, M. Yu., Kiselev, A. V., & Lobanov, N. A. (1979) *FEBS Lett. 100*, 219–224.

Pande, C., Callender, R. H., Chang, C.-H., & Ebrey, T. M. (1985) *Biophys. J. 42*, 549–552.

Pardoen, J. A., Winkel, C., Mulder, P. P. J., & Lugtenburg, J. (1984) *Recl. Trav. Chim. Pays-Bas 103*, 135–141.

Pardoen, J. A., van den Berg, E. M. M., Winkel, C., & Lugtenburg, J. (1985) *Recl. Trav. Chim. Pays-Bas 105*, 92–98.

Pines, A., Gibby, M. G., & Waugh, J. S. (1973) *J. Chem. Phys. 59*, 569–590.

Pnevmatikos, S. (1988) *Phys. Rev. Lett. 60*, 1534–1537.

Rothschild, K. J., & Marrero, H. (1982) *Proc. Natl. Acad. Sci. U.S.A. 79*, 4045–4049.

Scherrer, D., Mathew, M. K., Sperling, W., & Stoeckenius, W. (1989) *Biochemistry 28*, 829–834.

Sheves, M., Kohne, B., & Mazur, Y. (1983) *J. Chem. Soc., Chem. Commun.*, 1232–1234.

Smith, S. O., & Mathies, R. A. (1985) *Biophys. J. 47*, 251–254.

Smith, S. O., Pardoen, J. A., Lugtenburg, J., & Mathies, R. A. (1987) *J. Phys. Chem. 91*, 804–819.

Smith, S. O., de Groot, H. J. M., Gebhard, R., Courtin, J. M. L., Lugtenburg, J., Herzfeld, J., & Griffin, R. G. (1989) *Biochemistry 28*, 8897–8904.

Spudich, J. L., McCain, D. A., Nakanishi, K., Okabe, M., Shimizu, N., Rodman, H., Honig, B., & Bogomolni, R. A. (1986) *Biophys. J. 49*, 479–483.
Stoeckenius, W., & Bogomolni, R. A. (1982) *Annu. Rev. Biochem. 51*, 587–616.
Szundi, I., & Stoeckenius, W. (1987) *Proc. Natl. Acad. Sci. U.S.A. 84*, 3681–3684.
Szundi, I., & Stoeckenius, W. (1989) *Biophys. J. 56*, 369–383.
Tsironis, G. P., & Pnevmatikos, S. (1989) *Phys. Rev. B 39*, 7161–7173.

Spectral Perturbations and Oligomer/Monomer Formation in 124-Kilodalton *Avena* Phytochrome†

Jung-Kap Choi,‡ In-Soo Kim,§ Tae-Ik Kwon,‖ William Parker, and Pill-Soon Song*
Department of Chemistry and Institute for Cellular and Molecular Photobiology, University of Nebraska, Lincoln, Nebraska 68588-0304

Received January 29, 1990; Revised Manuscript Received March 26, 1990

ABSTRACT: We have studied the effects of pH, ionic strength, and hydrophobic fluorescence probes, 8-anilinonaphthalene-1-sulfonate (ANS) and bis-ANS, on the structure of intact (124-kDa) *Avena* phytochrome. The Pfr form of phytochrome forms oligomers in solution to a greater extent than the Pr form. Hydrophobic forces play a major role in the oligomerization of phytochrome, as suggested by fluorescence and monomerization by bis-ANS. However, electrostatic charges also take part in the phytochrome oligomerization. The partial proteolytic digestion patterns for the Pr and Pfr species are different, but binding of bis-ANS to the phytochrome abolishes this difference and yields an identical proteolytic peptide mapping for both spectral forms of phytochrome. This appears to result from bis-ANS binding at the carboxy-terminal domain, which induces monomerization of phytochrome oligomers. A second bis-ANS binding at an amino-terminal site blocks cleavage sites of trypsin and α-chymotrypsin. Bis-ANS especially blocks access of the proteases to the amino-terminal cleavage site that produces an early proteolytic product (114/118 kDa) on SDS gels. The bis-ANS binding does not, however, affect the proteolytic cleavage site that occurs in the hinge region between the two structural domains of phytochrome, the chromophore domain and the C-terminal non-chromophore domain. A chromophore binding site in the Pfr form is apparently exposed for preferential binding of bis-ANS, causing cyclization of the chromophore and bleaching of its absorbance at 730 nm. These observations have been discussed in terms of a photoreversible topographic change of the chromophore/apoprotein during the phototransformation of phytochrome.

Phytochrome is a chromoprotein consisting of a tetrapyrrole chromophore covalently linked to a polypeptide of molecular mass in the range of 120–127 kDa, depending upon plant species [for review, see Lagarias (1985) and Furuya (1987)]. Phytochrome exists in two forms that are photoreversible, with the Pr form absorbing maximally at 666 nm and the Pfr form at 730 nm. Photoconversion from the Pr to the Pfr form in vivo induces a number of photomorphogenic and developmental responses, including gene expression, whereas reversion of the Pfr to the Pr form cancels the induction of those responses [for review, see Pratt (1979), Schmidt and Mohr (1982), Song (1983), Quail (1984), Lagarias (1985), and Furuya (1987)].

On the basis of spectroscopic and ANS[1]-induced spectral bleaching studies on degraded 118/114-kDa oat phytochrome, a working model for the phytochrome phototransformation has been proposed (Song et al., 1979; Hahn & Song, 1981). According to the proposed model, the Pr to Pfr phototransformation generates a specific hydrophobic surface on the Pfr protein as a result of chromophore reorientation. The difference in hydrophobicity between the Pr and Pfr forms of 118/114-kDa phytochrome has been examined in terms of affinity for ANS (Hahn & Song, 1981), liposomes (Kim & Song, 1981), Cibacron blue F3GA (Smith & Daniels, 1981), and alkyl groups (Yamamoto & Smith, 1981).

However, the applicability of this model to native 124-kDa oat phytochrome (Vierstra & Quail, 1982, 1983) has not been examined. In fact, preliminary observations (Eilfeld & Ruediger, 1985) indicated that the spectroscopic behaviors of phytochrome, i.e., with respect to chromophore bleaching by ANS and tetranitromethane (Hahn et al., 1984), are significantly modulated by the presence of the 6/10-kDa amino-terminal fragment.

In this report, we describe a follow-up study of the structural properties of 124-kDa phytochrome as probed by bis-ANS. ANS and bis-ANS are unique fluorescence probes for the structural and topographical studies of the phytochrome molecule, not only because of their hydrophobic property (Brand & Gohlke, 1972) but more importantly due to their

† This work was supported by a grant from USPHS, NIH (GM36956), and by a grant from the Center of Biotechnology—University of Nebraska. I.-S.K. acknowledges the Korea Science and Engineering Foundation for a research grant.
* To whom correspondence should be addressed.
‡ Present address: College of Pharmacy, Chonnam National University, Kwangju, Korea.
§ Present address: Department of Genetic Engineering, Kyungpook National University, Taegu, Korea.
‖ Present address: Department of Biochemistry, Choongnam National University, Daejeon, Korea.

[1] Abbreviations: ANS, 8-anilinonaphthalene-1-sulfonate; bis-ANS, 4,4′-dianilino-1,1′-binaphthyl-5,5′-disulfonic acid dipotassium salt; CD, circular dichroism; CHAPS, 3-[(3-cholamidopropyl)dimethylammonio]-1-propanesulfonate; CTAB, cetyltrimethylammonium bromide; HA, hydroxylapatite; HPLC, high-performance liquid chromatography; KPB, potassium phosphate buffer; PAGE, polyacrylamide gel electrophoresis; PMSF, phenylmethanesulfonyl fluoride; SDS, sodium dodecyl sulfate.

0006-2960/90/0429-6883$02.50/0